Spatiotemporal patterning of IP_3-mediated Ca^{2+} signals in *Xenopus* oocytes by Ca^{2+}-binding proteins

Sheila L. Dargan[1], Beat Schwaller[2] and Ian Parker[1]

[1] *Department of Neurobiology and Behaviour, University of California Irvine, CA 92697-4550, USA*
[2] *Division of Histology, Department of Medicine, University of Fribourg, Switzerland*

Ca^{2+}-binding proteins (CaBPs) are expressed in a highly specific manner across many different cell types, yet the physiological basis underlying their selective distribution patterns remains unclear. We used confocal line-scan microscopy together with photo-release of IP_3 in *Xenopus* oocytes to investigate the actions of mobile cytosolic CaBPs on the spatiotemporal properties of IP_3-evoked Ca^{2+} signals. Parvalbumin (PV), a CaBP with slow Ca^{2+}-binding kinetics, shortened the duration of IP_3-evoked Ca^{2+} signals and 'balkanized' global responses into discrete localized events (puffs). In contrast, calretinin (CR), a presumed fast buffer, prolonged Ca^{2+} responses and promoted 'globalization' of spatially uniform Ca^{2+} signals at high [IP_3]. Oocytes loaded with CR or PV showed Ca^{2+} puffs following photolysis flashes that were subthreshold in controls, and the spatiotemporal properties of these localized events were differentially modulated by PV and CR. In comparison to results we previously obtained with exogenous Ca^{2+} buffers, PV closely mimicked the actions of the slow buffer EGTA, whereas CR showed important differences from the fast buffer BAPTA. Most notably, puffs were never observed after loading BAPTA, and this exogenous buffer did not show the marked sensitization of IP_3 action evident with CR. The ability of Ca^{2+} buffers and CaBPs with differing kinetics to fine-tune both global and local intracellular Ca^{2+} signals is likely to have significant physiological implications.

(Received 3 December 2003; accepted after revision 29 January 2004; first published online 30 January 2004)
Corresponding author I. Parker: Department of Neurobiology and Behaviour, University of California Irvine, CA 92697-4550, USA. Email: iparker@uci.edu

Cytosolic Ca^{2+} signals regulate cellular processes as diverse as fertilization, differentiation, synaptic plasticity and apoptosis. This versatility is possible because cells are equipped with a Ca^{2+} signalling 'toolkit' (Berridge *et al.* 2000), with many components (proteins) that can be selected to enable signalling over a wide range of different time and distance scales (Marchant & Parker, 2000). The most important components in the toolkit are the Ca^{2+} channels that generate intracellular Ca^{2+} signals; either by allowing Ca^{2+} influx across the plasma membrane, or by liberating Ca^{2+} from intracellular stores (through inositol 1,4,5-trisphosphate receptors (IP_3Rs) or ryanodine receptors (RyRs)). The majority of Ca^{2+} ions entering the cytosol are rapidly captured both by mobile cytosolic Ca^{2+}-binding proteins (CaBPs) and immobile buffers of unknown identity. In addition to simply reducing the availability of free cytosolic Ca^{2+} ions, immobile buffers reduce the effective diffusion coefficient for Ca^{2+}, whereas mobile buffers can act as a 'shuttle' to speed Ca^{2+} diffusion in the presence of immobile buffers (Stern, 1992; Roberts, 1994). It is thus likely that cells utilize CaBPs to shape Ca^{2+} signals for their specific functions; a notion supported by observations that different cell types – particularly subpopulations of neurones – selectively express mobile CaBPs with differing properties (Andressen *et al.* 1993).

CaBPs vary significantly in functional versatility, and are classified accordingly. 'Ca^{2+} sensors', such as calmodulin (Cheung, 1980; Vetter & Leclerc, 2003), undergo conformational changes on Ca^{2+} binding which enable them to bind to and activate target proteins to translate changes in intracellular [Ca^{2+}] into signalling cascades. On the other hand, 'Ca^{2+} buffers' such as parvalbumin (PV) and calretinin (CR) are thought to act solely to chelate Ca^{2+} ions – although this view may change as we learn more about their biology (Schwaller *et al.* 2002). Despite their apparent passive function, PV and CR have nevertheless generated great interest, mainly due to their

 DOI: 10.1113/jphysiol.2003.059204

exquisitely specific expression in certain subpopulations of nerve cells (Baimbridge *et al.* 1992; Andressen *et al.* 1993). In the cerebellum, for example, PV is present in Purkinje cells and a subpopulation of inhibitory interneurones (stellate and basket cells), whereas CR is mainly localized to granule cells and their parallel fibres (Schwaller *et al.* 2002). These selective distribution patterns provide an invaluable experimental tool for identifying subpopulations of neurones (antibodies against them are routinely used to stain for specific populations of nerve cells). However, the physiological basis underlying their specific expression patterns has remained largely elusive (Neher, 2000), although recent studies with knockout mice now point to specific roles for CaBPs in regulating Ca^{2+} pools essential for synaptic plasticity (Schwaller *et al.* 2002).

Most experimental and theoretical investigations regarding CaBPs have focused on their ability to modulate signals arising from Ca^{2+} influx through voltage-gated channels in the plasma membrane (Lee *et al.* 2000*a*,*b*; Meinrenken *et al.* 2003; Schmidt *et al.* 2003*b*). Actions of CaBPs on signals arising from Ca^{2+} release from intracellular stores (via IP_3Rs or RyRs) are likely to reflect a more complex situation (Dargan & Parker, 2003) because these release channels are themselves regulated by cytosolic $[Ca^{2+}]$, such that small increases in cytosolic $[Ca^{2+}]$ promote channel opening whereas higher concentrations are inhibitory (Iino, 1990; Finch *et al.* 1991; Bezprozvanny *et al.* 1991; Mak *et al.* 1998; Fill & Copello, 2002). Moreover, IP_3Rs are known to exist in clusters, comprising tens of channels, which act as functionally discrete Ca^{2+} release units (Callamaras *et al.* 1998*a*,*b*; Sun *et al.* 1998; Swillens *et al.* 1999). Clusters can operate autonomously to generate local signals (Ca^{2+} puffs) that arise because Ca^{2+}-induced Ca^{2+} release (CICR) leads to the near-simultaneous opening of multiple channels within a cluster (Yao *et al.* 1995; Bootman *et al.* 1997), and their activity can be synchronized by successive cycles of Ca^{2+} diffusion and CICR to generate Ca^{2+} waves that propagate in a saltatory manner across multiple clusters (Lechleiter & Clapham, 1992; Bootman *et al.* 1997; Berridge, 1997; Callamaras *et al.* 1998*a*,*b*; Dawson *et al.* 1999). Therefore, in addition to influencing the fate of Ca^{2+} ions already released into the cytosol, CaBPs are also likely to interfere with the Ca^{2+} feedback loops that act on very different distance and time scales to generate local signals by interactions between individual IP_3Rs, and on the cluster–cluster interactions responsible for transitioning from local to global modes of Ca^{2+} signalling.

We had previously studied these processes utilizing *Xenopus* oocytes as a model cell system in which to image perturbations of Ca^{2+} signalling resulting from intracellular injections of two synthetic buffers, EGTA and BAPTA (Dargan & Parker, 2003). The oocyte is a favourable system in which to study intracellular Ca^{2+} signals because Ca^{2+} liberation is mediated solely through type 1 IP_3Rs (Parys *et al.* 1992), its large size greatly facilitates intracellular injections and it is among the best characterized cells for Ca^{2+} signalling. Moreover, EGTA and BAPTA were selected because the Ca^{2+}-binding properties of these buffers are simple and well characterized and, while having similar affinities, they show very different binding kinetics. Our main findings were that the 'slow' buffer EGTA accelerates the time course of IP_3-evoked Ca^{2+} signals and dissociates global Ca^{2+} waves into autonomous local release events, whereas the 'fast' buffer BAPTA results in 'globalization' of spatially diffuse, and slowly decaying Ca^{2+} signals. These actions were attributed to the differential effects of buffers with differing kinetics on Ca^{2+} interactions between individual IP_3Rs within a cluster, and on interactions between neighbouring clusters.

In the present paper we extend these studies to the more complex CaBPs expressed endogenously within cells. PV and CR were selected for these experiments because they show cell-specific expression and have contrasting Ca^{2+}-binding kinetics. Under physiological conditions PV acts as a slow buffer, because its binding sites are predominantly occupied by Mg^{2+} ions which must be displaced before Ca^{2+} can bind (Haiech *et al.* 1979; Eberhard & Erne, 1994). CR is less well characterized, but functions as a fast intracellular buffer (Edmonds *et al.* 2000) analogous to BAPTA. We show that the 'slow' CaBP (PV) closely mimics the actions of EGTA, by speeding IP_3-evoked Ca^{2+} transients and 'balkanizing' global Ca^{2+} waves into local puffs. On the other hand, the 'fast' CaBP (CR) has more complex actions. High concentrations of CR result in spatially diffuse, slowly decaying Ca^{2+} signals similar to the action of BAPTA; but, different to BAPTA, CR sensitizes responses to IP_3 and low concentrations of CR actually promote local puffs. The ability of CaBPs to specifically modulate both local and global intracellular Ca^{2+} signals is likely to have significant physiological implications.

Methods

Preparation of *Xenopus* oocytes

Xenopus laevis (purchased from Nasco International, Fort Atkinson, WI, USA) were anaesthetized by immersion in 0.17% MS-222 for 15 min and killed by decapitation in adherence with protocols approved by the UC Irvine Institutional Animal Care and Use Committee. Stage

V–VI oocytes were manually plucked, collagenase-treated (0.5 mg ml^{-1} for 30 min) and stored in modified Barth's solution (mM: NaCl, 88; KCl, 1; $NaHCO_3$, 2.4; $MgSO_4$, 0.82; $Ca(NO_3)_2$, 0.33; $CaCl_2$, 0.41; Hepes, 5; gentamicin, 0.1 mg ml^{-1}; pH 7.4) for 1–7 days before use.

Preparation of Ca^{2+}-binding proteins and injection solutions

Human recombinant CR containing a 6xHis tag on the N-terminus was produced in *E. coli* as previously described (Schwaller *et al.* 1997), and the overexpressed protein was purified on a nickel chelate column. The 6xHis tag does not appear to influence the Ca^{2+}-binding affinities of CR (B. Schwaller, unpublished observation). After dialysis, CR was lyophilized from 50 μl of a solution containing (mM): $(NH_4)HCO_3$, 5; $CaCl_2$, 1; (β-mercaptoethanol, 1 and DTT, 1. Neither $(NH_4)HCO_3$ nor (β-mercaptoethanol were expected to be present in the injection solution since they are both volatile and would have evaporated during lyophilization. However, CR in the injection solution was expected to be in its Ca^{2+}-bound form. Experiments to control for the presence of Ca^{2+} and DTT in the CR injection solution are presented in Results. Recombinant rat PV was produced in *E. coli*, purified by chromatographic methods as previously described (Pauls *et al.* 1993) and lyophilized after desalting on a spin column. Thus the PV-containing injection solution did not contain any salts beyond those listed below. Lyophilized CaBPs were dissolved in 250 mM KCl, 10 mM Hepes to give 1 mM stock injection solutions, which were aliquotted into small volumes each sufficient for one experiment, and stored at –20°C until use.

Microinjection of oocytes

Intracellular microinjections were performed using a Drummond microinjector, and final intracellular concentrations were calculated assuming a 1 μl cytosolic volume. Oocytes were initially loaded with OG-1 (Oregon Green 488 BAPTA-1) and caged-IP_3 (D-*myo*-inositol 1,4,5-trisphosphate, $P_{4(5)}$-(1-(2-nitrophenyl)ethyl) ester) to final intracellular concentrations of 48 and 8 μM, respectively. Control Ca^{2+} responses were imaged, after allowing 30 min for intracellular distribution. A specified volume of CaBP-containing solution was then injected through a fresh micropipette that was removed immediately to minimize leakage, and Ca^{2+} responses were imaged after allowing > 15 min for intracellular equilibration of [CaBP]. Sequential injections and recordings were made in this way to examine the effects of stepwise increases in [CaBP]. For the experiments studying local events (Fig. 6) oocytes were loaded with Fluo-4-dextran (low affinity version: 25 μM final intracellular concentration), caged-IP_3 (12 μM), and either PV (100 μM) or CR (100 μM); and were imaged 1.5 h later, to allow for slow diffusion of dextran-conjugated Fluo-4.

Confocal laser scanning microscopy

Confocal Ca^{2+} images were obtained as previously described (Dargan & Parker, 2003), using a custom-built line-scan confocal scanner interfaced to an Olympus IX70 inverted microscope (Parker *et al.* 1997). Images were collected using custom-written image acquisition software (Labview). Recordings were made at room temperature, imaging at the level of the pigment granules in the animal hemisphere of oocytes bathed in normal Ringer solution (composition (mM): $NaCl_2$, 120; KCl, 2; $CaCl_2$, 1.8; Hepes, 5; pH 7.3). Images in figures are representative confocal recordings acquired at a scan rate of 16 ms $line^{-1}$ (except Fig. 6, acquired at 2.6 ms $line^{-1}$). IP_3 was uniformly photo-released throughout a 200 μm spot surrounding the image scan line (Callamaras & Parker, 1998), and [IP_3] was controlled (in a linear manner) by using an electronic shutter to vary flash duration. Since each flash consumes only a negligible fraction of the caged IP_3 (Callamaras & Parker, 1998), numerous consistent responses could be acquired using repeated flashes. Intervals of > 60 s were allowed between recordings for IP_3Rs to recover from desensitization and for cytosolic [Ca^{2+}] to recover to basal levels. Fluorescence signals are expressed as ratios (F/F_0 or $\Delta F/F_0$) of the fluorescence (F) at each pixel relative to the mean resting fluorescence (F_o) at that pixel prior to stimulation. Flash durations are normalized relative to that evoking a half-maximal response under control conditions in each cell, to control for variation between oocytes. Custom routines written in the IDL programming environment (Research Systems, Boulder, CO, USA) were used for image processing and measurements were exported to Microcal Origin version 6.0 (OriginLab, Northampton, MA, USA) for analysis and graphing.

Derivation of calcium flux

To estimate the kinetics of Ca^{2+} flux from into the cytosol through IP_3Rs (Fig. 4) we assumed that that subsequent Ca^{2+} clearance follows a first order process (Parker *et al.* 1996) with a rate constant (k; 0.95 s^{-1}) corresponding to that previously measured from the decay of Ca^{2+} signals following influx through N-type channels (Dargan &

Parker, 2003). The rate of Ca^{2+} efflux (E) from intracellular stores is thus proportional to

$$E \sim d[Ca^{2+}]/dt + k[Ca^{2+}]$$

where $[Ca^{2+}]$ is the free Ca^{2+} level as signalled by the fluorescence. Traces of Ca^{2+} flux through IP_3Rs (Fig. 4*B*) were calculated from this equation by numerical differentiation of the 'raw' fluorescence traces (Fig. 4*A*) after smoothing by a 15 point running average to reduce noise.

Reagents

Oregon Green 488 BAPTA-1, caged IP_3 and Fluo-4-dextran (low affinity version, $K_d = 4\ \mu M$) were purchased from Molecular Probes Inc. (Eugene, OR, USA); all other reagents were from Sigma Chemical Co. (St Louis, MO, USA).

Results

Modulation of IP_3-evoked Ca^{2+} signals by mobile CaBPs

We compared the actions of two mobile CaBPs with differing Ca^{2+} binding kinetics, PV and CR, on IP_3-evoked intracellular Ca^{2+} signals in *Xenopus* oocytes. Figures 1 and 2 illustrate our basic experimental protocol. Ca^{2+} images were acquired at various concentrations of CaBPs in response to a fixed flash duration (Fig. 1) or series of flash durations (Fig. 2). Following acquisition of control records (top panels: Figs 1 and 2), a specified volume of a CaBP-containing solution (PV; Figs 1*A* and 2*A*: CR; Figs 1*B* and 2*B*) was injected into the oocyte to give a final intracellular concentration of 25 μM (see Methods for details). Microinjection pipettes were removed immediately following injection, to prevent leakage, and the oocytes were left for ~20 min to allow for uniform CaBP distribution. Ca^{2+} signals were then imaged in response to the same series of UV flashes. Subsequent injections were made following the same protocol to image IP_3-evoked Ca^{2+} signals at various cytosolic CaBP concentrations ranging from 50 to 250 μM.

The data in Figs 1 and 2 are representative of observations in 37 oocytes (PV $n = 18$; CR $n = 19$). The results are analysed in the following sections, but the most striking findings were that the 'slow' CaBP PV greatly abbreviated IP_3-evoked Ca^{2+} signals and 'balkanized' global responses into discrete localized events, whereas the 'fast' CaBP CR slowed the decay of IP_3-evoked Ca^{2+} signals and, at high concentrations, promoted spatially uniform responses.

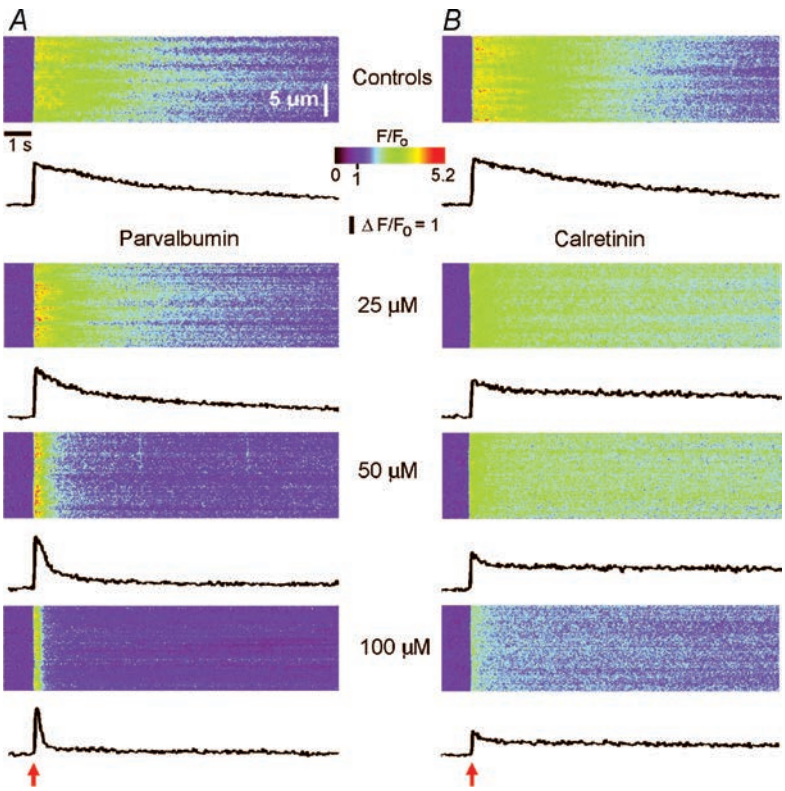

Figure 1. Parvalbumin (PV) and calretinin (CR) modulate IP_3-evoked Ca^{2+} signals
Confocal line-scan images from two oocytes illustrate Ca^{2+} signals evoked by photoreleased IP_3 in the presence of increasing [PV] or [CR]. Data are representative of similar findings in 37 oocytes (PV, $n = 18$; CR, $n = 19$). Identical photolysis flashes (normalized durations of 1.4 in *A* and 1.7 in *B*) were delivered at the arrows. Traces below each image show fluorescence profiles averaged over 21 pixels (1.4 μm) regions. *A*, top panel shows control response prior to loading buffer, and subsequent panels illustrate responses after sequentially loading the same oocyte with PV to the final intracellular concentrations stated. *B*, similar records from a different oocyte showing the effects of increasing concentrations of CR.

Differential actions of 'slow' and 'fast' CaBPs on the decay of IP_3-evoked Ca^{2+} signals

In control conditions (before loading any CaBPs), IP_3-evoked Ca^{2+} transients decayed mono-exponentially with a time constant of a few seconds that slowed progressively with increasing photo-release of IP_3 (Fig. 2*A*, top panels). In the presence of increasing [PV] the decay of IP_3-evoked Ca^{2+} signals became markedly biphasic, with a prominent fast component and a smaller slower component. CR also induced bi-exponential decay, but in this case the slow-phase was more pronounced and the fast component became smaller with increasing [CR]. These actions are more clearly evident in Fig. 2*B*, showing superimposed responses to strong photolysis flashes in the presence of increasing [PV] or [CR] after normalizing amplitudes to facilitate comparison of their respective kinetics.

Facilitation and depression of IP_3-evoked Ca^{2+} signals by 'slow' CaBPs

Figure 3*A* and *B* shows the mean peak amplitude of fluorescence signals at various concentrations of PV and CR, respectively, plotted as a function of increasing photo-release of IP_3 (expressed as normalized flash duration; see Methods). These data are fitted by the Hill equation: $y = V_{max}\ (x^{nH}/(EC_{50}{}^{nH} + x^{nH}))$, where y is the peak fluorescence ratio ($\Delta F/F_o$) at any given [IP_3] (x); V_{max} is the peak $\Delta F/F_o$ at saturating [IP_3]; n_H is the Hill coefficient, a measure of the apparent cooperativity of IP_3 action in evoking Ca^{2+} liberation; and the EC_{50} is the normalized [IP_3] evoking a half-maximal response. Parameters generated from these Hill fits are plotted in Fig. 3*C–E* to show the dependence of V_{max} (Fig. 3*C*), n_H (Fig. 3*D*) and EC_{50} (Fig. 3*E*) on [PV] (○) and [CR] (■).

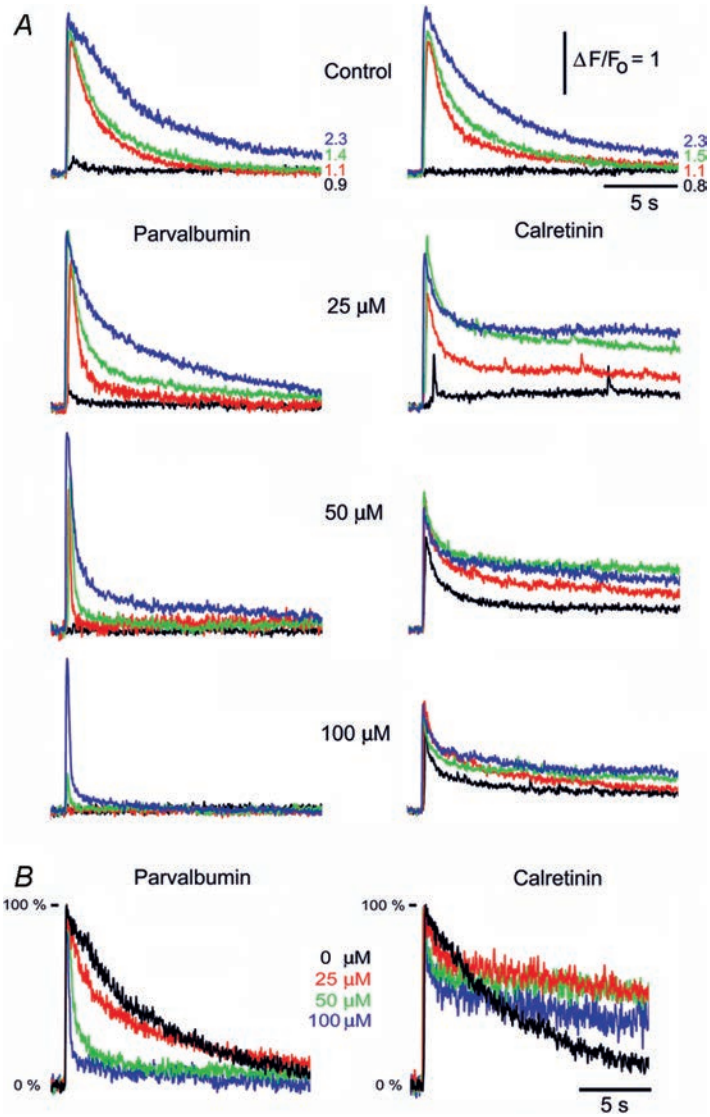

Figure 2. Parvalbumin and calretinin differentially modulate the decay kinetics of IP_3-evoked Ca^{2+} transients
A, buffer actions at varying [IP_3]. Representative fluorescence profiles show superimposed Ca^{2+} transients evoked by increasing photorelease of IP_3 in the absence of exogenous CaBP (top panels) and after loading increasing concentrations of PV (left) or CR (right). Traces correspond to different photolysis flash durations, indicated in normalized units. *B*, Ca^{2+} transients are shortened by PV but prolonged by CR. Families of curves illustrating Ca^{2+} transients evoked by a fixed photolysis flash in the presence of the indicated concentrations of PV (left) and CR (right) (normalized flash durations were 1.4 and 1.7, for PV and CR, respectively). Responses are scaled to same peak height to facilitate comparison of kinetics.

Increasing concentrations of CR caused a progressive reduction of Ca^{2+} signals evoked by strong photorelease of IP_3 (Fig. 3*B*) and V_{max} was correspondingly reduced (Fig. 3*C*). This is expected, in part simply because the added CaBP will compete with the indicator dye for free Ca^{2+} ions. However, this trend was not observed with increasing concentrations of PV. Rather, the amplitude of Ca^{2+} signals evoked by high [IP_3] was modulated in a biphasic manner, with an initial potentiation at 25 μM, and depression at [PV] > 100 μM (Fig. 3*A*). This is illustrated more clearly in Fig. 3*C*, showing enhancement of V_{max} at low [PV].

Although CR reduced V_{max} (Fig. 3*C*), responses to weak flashes were potentiated (Fig. 3*B*). This arose as the result of a marked leftward shift in the concentration–response relationship, such that the EC_{50} (normalized flash duration evoking a half-maximal signal) was reduced by about 55% with 100 μM CR (Fig. 3*E*). In contrast, the potentiation seen with PV involved only an increase in V_{max}, while the EC_{50} remained almost unchanged (Fig. 3*E*).

In contrast to the PV-containing injection solution (which comprised only PV, together with 250 mM KCl and 10 mM Hepes), the CR-containing injection solution additionally contained DTT and Ca^{2+} (see Methods). To assess whether these may have influenced the results obtained with CR we performed control experiments comparing IP_3-evoked Ca^{2+} signals before and after loading DTT to an equivalent final intracellular concentration (75 μM). No appreciable differences were observed (V_{max} decreased by 5.2 ± 6.7%; EC_{50} increased by 11.3 ± 4.5%: $n = 8$ oocytes, 2 frogs). Moreover, little change was apparent when oocytes were loaded with Ca^{2+} (50 nl of 1.5 mM $CaCl_2$) together with DTT (V_{max} increased by 5.9 ± 4.1%; EC_{50} increased by 4 ± 7%: $n = 6$ oocytes, 2 frogs).

CaBPs reduce the apparent cooperativity of IP_3-evoked Ca^{2+} liberation

Control oocytes (without added buffer) displayed a strongly cooperative Hill coefficient (n_H ~9). This value is greater than expected even if the opening of the IP_3R channel requires IP_3 binding to all four subunits, and is likely to reflect both the requirement for IP_3-binding to more than one subunit, together with a positive

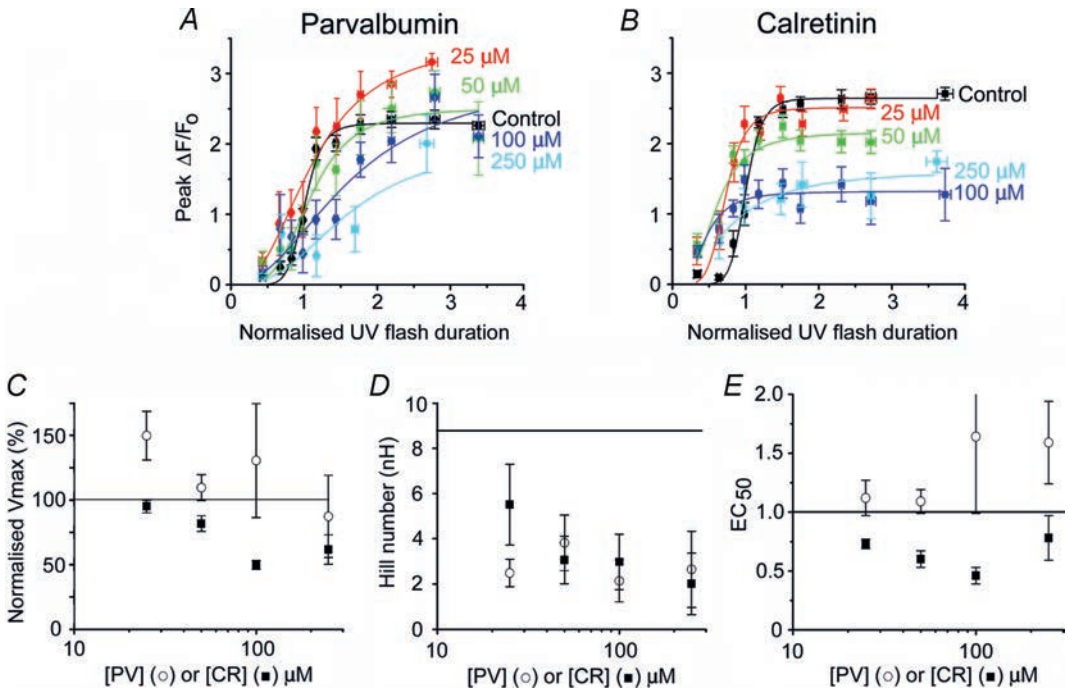

Figure 3. CaBPs modulate the concentration–response relationship of IP_3-evoked Ca^{2+} signals
A and *B*, mean peak amplitude ($\Delta F/F_0$) of Ca^{2+} signals as a function of normalized photolysis flash duration, plotted for various intracellular concentrations of PV (*A*: $n = 16$ oocytes) and CR (*B*: $n = 18$ oocytes). Curves were fitted using the Hill equation. *C–E*, parameters derived from Hill fits to the concentration–response relationships. In each panel, ○ represent values derived at different concentrations of PV, and ■ show corresponding values for CR. Horizontal lines represent control values (i.e. before loading CaBP). *C*, V_{max} (maximal fluorescence signal at infinite [IP_3]) as a function of [CaBP]. *D*, Hill coefficients (n_H) as functions of [CaBP]. *E*, EC_{50} as a function of [CaBP].

cooperativity resulting from CICR (Meyer *et al.* 1990; Hirota *et al.* 1995; Marchant & Taylor, 1997; Callamaras *et al.* 1998*a*). Consistent with this, the Hill coefficient declined progressively with increasing concentrations of PV and CR; probably because CaBPs disrupt Ca^{2+} diffusion between IP_3Rs that ordinarily leads to CICR and contributes appreciably to the apparent cooperativity of IP_3 action (Dargan & Parker, 2003). The minimal n_H ($\sim$2) obtained in the presence of high concentrations of PV and CR suggests that the binding of two (or possibly even one) molecules of IP_3 to each tetramer is sufficient for channel opening. Moreover, a low concentration (25 μM) of PV caused a greater reduction in n_H than the same concentration of CR (Fig. 3*D*).

Biphasic Ca^{2+} liberation through IP_3Rs

To further elucidate the actions of CaBPs on the kinetics of Ca^{2+} signals, we attempted to derive the changes in underlying Ca^{2+} flux through IP_3Rs. The time course of cytosolic [Ca^{2+}] reflects a balance between Ca^{2+} liberation through the IP_3R and the subsequent clearance of free Ca^{2+} ions from the cytosol by chelation, re-sequestration and extrusion. We estimated the release flux based on previous findings that cytosolic Ca^{2+} clearance in the oocyte can be approximated as a first order process with a rate constant (k) of about 0.95 s^{-1} (Parker *et al.* 1996: Dargan & Parker, 2003). The kinetics of Ca^{2+} flux into the cytosol through IP_3Rs will thus be proportional to $d[Ca^{2+}]/dt + k[Ca^{2+}]$, where [$Ca^{2+}$] is the free cytosolic Ca^{2+} level as signalled by changes in fluorescence ($\Delta F/F$).

Figure 4 shows representative traces of 'raw' fluorescence signals (*A*) and derived Ca^{2+} flux rates (*B*) under control conditions and after intracellular loading of 100 μM PV or CR. Consistent with previous observations (Parker *et al.* 1996; Dargan & Parker, 2003), IP_3-evoked Ca^{2+} flux in control oocytes was characterized by an initial fast spike followed by a lingering 'tail' that persisted for several seconds (Fig. 4*B*, top panel). Despite its low amplitude, this tail component contributes significantly to the total amount of liberated Ca^{2+}, and is responsible for the prolonged Ca^{2+} transients evoked by IP_3 under normal conditions (Parker *et al.* 1996; Dargan & Parker, 2003). PV abolished the tail component (Fig. 4*B*, middle panel), whereas the same concentration of CR did not Fig. 4*B*, bottom panel). These findings mirror our earlier results with EGTA and BAPTA (Dargan & Parker, 2003) in showing that prolonged release of Ca^{2+} through the IP_3R is selectively disrupted by slow buffers.

'Fast' and 'slow' CaBPs differentially alter the spatial distribution of Ca^{2+} signals

Control oocytes without added CaBPs often display localized Ca^{2+} signals (puffs) within a narrow range of flash durations (Yao *et al.* 1995); but, as was the case in Fig. 5, it is sometimes possible to evoke only spatially diffuse Ca^{2+} waves (Fig. 5*A*). Following injection of 100 μM PV, the same oocytes displayed discrete localized puffs with flash durations that were too brief to evoke detectable responses under control conditions (top panels, Fig. 5*A* and *B*: representative of 9 oocytes). Moreover, following strong flashes, PV 'balkanized' global signals into localized release events (middle panel, Fig. 5*B*), which arose synchronously at higher [IP_3] generating the abrupt, rapidly decaying Ca^{2+} transients previously described (bottom panels, Figs 5*B* and 1*A*). Puffs observed following this initial

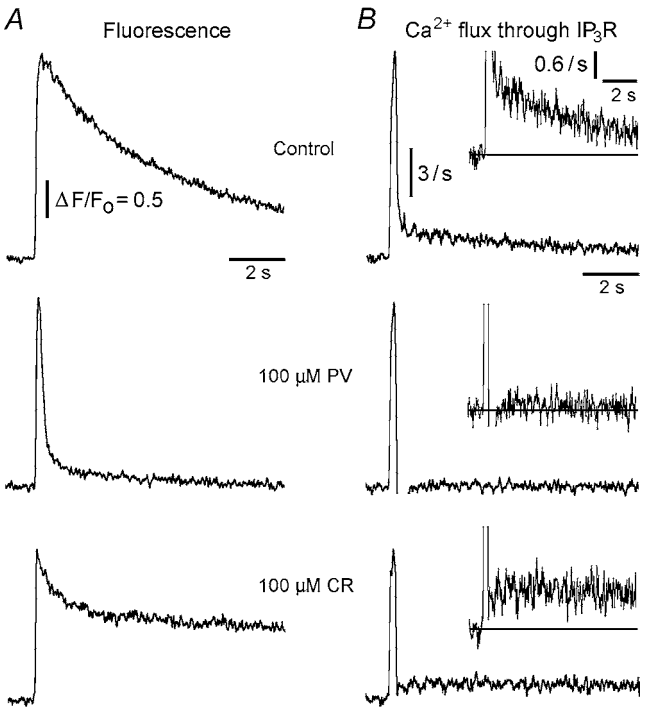

Figure 4. Biphasic Ca^{2+} liberation through IP_3Rs, and selective reduction of the slow component of Ca^{2+} release by parvalbumin

A, representative fluorescence signals evoked by photoreleased IP_3 in control conditions (top), and in the presence of 100 μM PV (middle) or 100 μM CR (bottom). *B*, rates of Ca^{2+} flux into the cytosol derived from the records in *A*, assuming that cytosolic Ca^{2+} clearance follows a first order process with a time constant of about 1 s (see text for further details). Traces were smoothed using 15 point adjacent averaging. The vertical calibration bars correspond to a rate of increase in fluorescence ($d(\Delta F/F_o)/dt$). Control traces (in *A* and *B*) are from the same oocyte as the CR traces. The fluorescence trace for the PV-paired control (not shown) was closely similar to that of the CR-paired control.

transient were asynchronous, and increased in frequency with progressively stronger stimuli.

In contrast to the uniform balkanizing action of PV, the spatial patterning of Ca^{2+} signals was modulated in a more complex, concentration-dependent manner by CR. Photolysis flashes that were subthreshold in control oocytes evoked Ca^{2+} puffs in the presence of 100 μM CR (Fig. 5*C*, top panel: representative of 9 oocytes). However, at higher $[IP_3]$ CR-loaded oocytes showed spatially uniform, slowly decaying Ca^{2+} signals (Fig. 5*C*, bottom two panels).

CaBPs modulate the spatiotemporal properties of Ca^{2+} puffs

Ca^{2+} puffs arise from autonomous activation of individual clusters of IP_3Rs. The fact that both PV and CR promoted the appearance of Ca^{2+} puffs thus allowed us to investigate their respective effects on the interactions between IP_3Rs within a cluster while excluding the cluster–cluster interactions that lead to global waves. For these experiments we selected oocytes that showed puffs in the absence of added CaBP, and imaged using the Ca^{2+} indicator dye Fluo-4-dextran which shows a greater (~15-fold) Ca^{2+}-dependent fluorescence increase as compared to Oregon Green, whilst obviating the rapid compartmentalization experienced with free Fluo-4. Figure 6 shows averaged confocal line-scan images of Ca^{2+} puffs ($n = 18$ events for each image) evoked in control, PV- and CR-containing oocytes, together with corresponding traces of fluorescence amplitude measured at the centre of each event. The time course of puff termination was determined by fitting single or double exponential curves (red) to the decay of averaged fluorescence profiles. In control oocytes the mean decay followed a bi-exponential curve, with an initial rapid decline ($\tau = 65$ ms) followed by a slow tail ($\tau = 809$ ms). PV (50 μM) almost completely abolished this tail component, while having little effect on the initial fast decay ($\tau = 67$ ms). CR (50 μM) slightly accelerated the fast decay ($\tau = 48$ ms), while slightly slowing the tail ($\tau = 967$ ms) component, as compared to control. In all conditions, the decay of Ca^{2+} signals during puffs was faster than the corresponding decay of global Ca^{2+} signals; this was probably due, at least in part, to the rapid diffusional dissipation of Ca^{2+} ions from the localized release source at a puff site. CaBPs therefore not only differentially modulate global responses

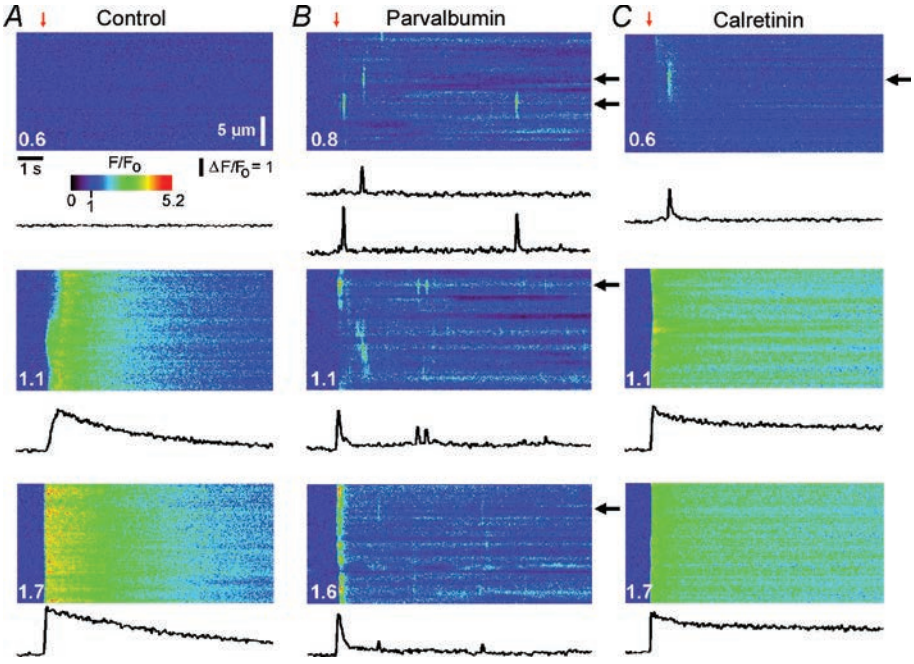

Figure 5. Parvalbumin 'balkanizes' Ca^{2+} signals into discrete, autonomous units, whereas calretinin promotes spatially uniform global signals

A, line-scan images and fluorescence profiles (averaged over 4 μm regions) showing responses to photolysis flashes (red arrows) of increasing duration (indicated in normalized units) before injecting buffer. *B*, corresponding records in a different oocyte after loading 100 μM PV (records in this oocyte before loading PV were similar to those in *A*). Two representative fluorescence profiles are illustrated from each image, recorded at different puff sites (black arrows). *C*, corresponding records after loading with 100 μM CR, from the same oocyte as in *A*.

(Fig. 1) but can additionally shape local IP_3-evoked Ca^{2+} signals.

Discussion

IP_3Rs are distributed in clusters (comprising tens of channels) spaced a few micrometres apart in the cytoplasm of cells ranging from *Xenopus* oocytes (Callamaras *et al.* 1998*a*,*b*; Swillens *et al.* 1999; Shuai & Jung, 2002, 2003) to various mammalian cell lines (Bootman *et al.* 1997; Simpson *et al.* 1997). CICR between IP_3Rs can thus act over two very different spatiotemporal scales: fast diffusion of Ca^{2+} over short (nm) distances within a release site to generate local Ca^{2+} puffs, and slower diffusion between neighbouring clusters (μm scale) to generate propagating saltatory waves (Yao *et al.* 1995; Bootman *et al.* 1997; Berridge, 1997; Callamaras *et al.* 1998*a*,*b*; Marchant & Parker, 2000). Intracellular Ca^{2+} buffers with differing kinetics are likely to exert complex actions on IP_3-evoked Ca^{2+} signalling, by differentially modulating one, or both, of these CICR processes. To study these actions we measured the effects of injecting exogenous buffers into *Xenopus* oocytes. A complication of this approach is that little is known regarding the nature and properties of the endogenous buffers already present in the oocyte. However, the finding that the addition of small amounts of exogenous buffer (e.g. an intracellular concentration of 25 μM parvalbumin) produced large effects on Ca^{2+} signals suggests that only low levels of endogenous mobile buffer are present, and would not appreciably affect our results at higher concentrations of added buffers. We had previously investigated two exogenous buffers, EGTA and BAPTA, since they have simple and well-characterized binding properties and have similar affinities yet very different kinetics (Dargan & Parker, 2003). The results and working model that emerged from that study now provide a framework for our analysis of the two endogenous CaBPs PV and CR which, in contrast to EGTA and BAPTA, contain multiple Ca^{2+}-binding sites and exhibit more complex Ca^{2+}-binding properties in terms of both kinetics and binding affinities.

Spatiotemporal patterning of Ca^{2+} signals is differentially modulated by fast and slow exogenous buffers

The main findings from our previous study (Dargan & Parker, 2003) were that EGTA (a 'slow' Ca^{2+} buffer) caused IP_3-evoked Ca^{2+} signals to become more transient, and 'balkanized' Ca^{2+} liberation such that individual release sites functioned autonomously to generate discrete puffs, whereas BAPTA (a 'fast' Ca^{2+} buffer) prolonged IP_3-evoked Ca^{2+} responses and promoted 'globalization' of spatially uniform Ca^{2+} signals. These strikingly distinct actions were not due to chelation of Ca^{2+} subsequent to its liberation into the cytosol, changes in resting free $[Ca^{2+}]$ or alterations in Ca^{2+} store filling. Instead, EGTA and BAPTA are likely to act over different time and distance scales to modulate the processes of Ca^{2+} diffusion and CICR that shape the regenerative nature of IP_3-evoked Ca^{2+} liberation. We previously proposed that slow Ca^{2+} buffers bind Ca^{2+} ions diffusing over the micrometer distances between neighbouring clustered release sites, render this Ca^{2+} unavailable for further CICR, and 'shuttle' it long distances before 'dumping' Ca^{2+} ions deep in the interior of the oocyte where release sites are absent (Dargan & Parker, 2003). The overall action of slow buffers is thus to disrupt intercluster Ca^{2+} communication, sharply restricting Ca^{2+} signals around individual release sites, whilst sparing short-range Ca^{2+} feedback. We additionally proposed that fast buffers may bind Ca^{2+} ions diffusing over nanometer distances to disrupt CICR between individual receptors within clusters. Ca^{2+} bound to fast buffers is rapidly (~10 ms)

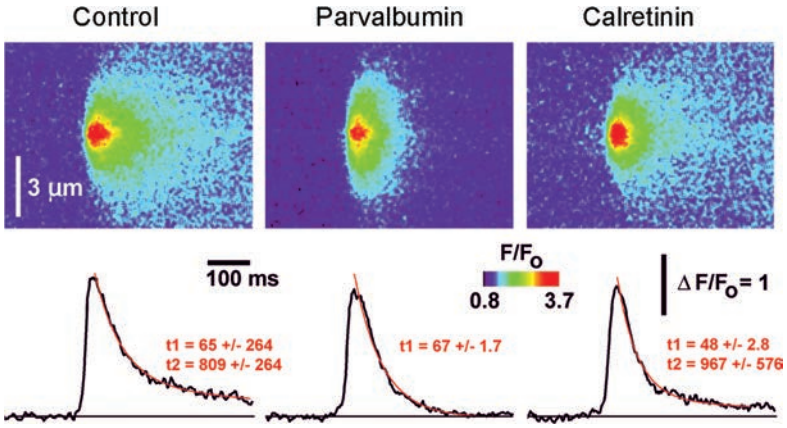

Figure 6. IP_3-evoked Ca^{2+} puffs terminated more rapidly in the presence of parvalbumin
Averaged line-scan images ($n = 18$ events for each) and their corresponding fluorescence profiles (averaged over 0.6 μm regions) of Ca^{2+} puffs evoked by low photo-release of IP_3 in the absence of added buffer (left panel) and in the presence of 50 μM PV (centre panel) or 50 μM CR (right panel). Images were acquired at a scan rate of 2.6 ms $line^{-1}$ using the indicator dye Fluo-4-dextran (low affinity version). Red curves represent single (for PV oocyte) or double (for control and CR-containing oocyte) exponential fits to the decay phase of puffs.

Table 1. Summary of kinetic parameters and diffusion distances for binding and unbinding of Ca^{2+} to EGTA, BAPTA, PV and CR

	'Slow' buffers		'Fast' buffers	
	EGTA	PV	BAPTA	CR
Ca^{2+} sites (functional)	1 (1)	3 (2)	1 (1)	6 (5)
App. K_d (nM) (pH 7.2)	150	150 *	160	1500 **
k_{on} ($\mu M^{-1}s^{-1}$)	3–10	6 *	100–1000	100–1000 ***
k_{off} (s^{-1})	0.5–1.5	0.9	16–160	150–1500
τ_{dwell} (ms)	700–2000	1050	6–60	0.7–7
$D_{Cabuffer}$ ($\mu m^2 s^{-1}$)	200	43	200	< 40
$d_{shuttle}$ (μm)	28–50	16	3–9	0.4–1.3
$\tau_{capture}$ (ms)	4–10	3	0.04–0.4	0.007–0.07
	([B] = 270 μM)	([B] = 540 μM)	([B] = 270 μM)	([B] = 1.35 mM)
$d_{capture}$ (μm)	0.7–1	0.4	0.07–0.2	0.03–0.09
	([B] = 270 μM)	([B] = 540 μM)	([B] = 270 μM)	([B] = 1.35 mM)

Values were taken from published literature where possible. Other values were assumed or derived as described below. On- and off-rates were derived assuming $k_{off} = K_d k_{on}$. Dwell times (τ_{dwell}), reflecting how long Ca^{2+} will remain bound to each buffer, equal $1/k_{off}$. The corresponding mean distances over which the Ca^{2+}buffer complexes will diffuse before releasing bound Ca^{2+} ($d_{shuttle}$) were estimated as $\sqrt{(D_{Cabuffer}\tau_{dwell})}$. $D_{Cabuffer}$ is 43 μm^2 s^{-1} for PV (Schmidt *et al.* 2003*a*) and estimated to be < 40 μm^2 s^{-1} for CR based on the $D_{Cabuffer}$ value of the closely related protein calbindin D-28k (H. Schmidt, unpublished observation). $d_{shuttle}$ for CR was calculated assuming $D_{Cabuffer} = 40$. Mean capture times before a Ca^{2+} ion binds to PV or CR were calculated from $\tau_{capture} = 1/(k_{on}[B])$ (Stern, 1992; Roberts, 1994), where [B] is the concentration of Ca^{2+}-free binding sites on the buffer, assuming that Ca^{2+} ions in the cytosol are bound to immobile endogenous buffers for 90% of the time. Corresponding mean capture distances were estimated using the relation $d_{capture} = \sqrt{6 D_{Ca} \tau_{capture}}$, assuming an apparent diffusion coefficient (D_{Ca}) of 20 μm^2 s^{-1} for Ca^{2+} in the presence of immobile endogenous buffers. * K_d and k_{on} for PV are highly dependent on $[Mg^{2+}]$ – the values stated (Schwaller *et al.* 2002) are estimates at physiological cytosolic $[Mg^{2+}]$ (0.6–0.9 mM). ** CR has multiple sites with different K_d values – the half-saturation value is shown ($[Ca^{2+}]_{50} = 1500$ nM) (Schwaller *et al.* 1997). *** The stated k_{on} for the 'fast' binding site(s) of CR as estimated by Edmonds *et al.* (2000) was used to derive the other kinetic parameters. More recent data (G. Faas, unpublished observations) suggests that the multiple sites of CR have differing kinetics.

'shuttled' a few micrometres, a distance comparable to intercluster spacing, before it dissociates. In this manner, fast buffers may act to inhibit *intra*cluster feedback by Ca^{2+} whilst simultaneously facilitating *inter*cluster Ca^{2+} communication.

Ca^{2+}-binding properties of PV and CR *versus* EGTA and BAPTA

Table 1 lists key factors determining the interactions of Ca^{2+} ions with PV and CR and, for comparison, with EGTA and BAPTA. Parameters include: (1) the mean time for which a Ca^{2+} ion will diffuse ($\tau_{capture}$) and the distance ($d_{capture}$) that it will diffuse before it becomes bound to a buffer molecule; (2) the mean time (dwell time; τ_{dwell}) for which a Ca^{2+} ion will remain bound to a buffer before dissociating, and the corresponding mean distance ('shuttle' distance; $d_{shuttle}$) that the Ca^{2+}–buffer complex will diffuse before dissociation. Further, diffusion of Ca^{2+} ions in the cytosol is slowed by binding to endogenous, immobile buffers. Less than 10% of the total Ca^{2+} ions in the cytosol are free at any given time, and the apparent diffusion coefficient for Ca^{2+} in the oocyte is thereby slowed about 10-fold as compared to free aqueous diffusion (20 μm^2 s^{-1} *versus* 200 μm^2 s^{-1}, respectively; Allbritton *et al.* 1992; Yao *et al.* 1995). PV is freely mobile in the cytosol (Schmidt *et al.* 2003*a*), and can therefore act to speed or facilitate Ca^{2+} transport by shuttling bound Ca^{2+} ions through this 'forest' of immobile buffers (Stern, 1992; Roberts, 1994). When calculating parameters for CR (Table 1) we assumed that CR is similarly mobile (Edmonds *et al.* 2000). However, other reports indicate that some CR molecules may bind in a Ca^{2+}-dependent manner to membrane constituents (Winsky & Kuznicki, 1995; Hubbard & McHugh, 1995).

Under physiological intracellular conditions PV acts as a 'slow' CaBP, because its two functional EF hands ('mixed' Ca^{2+}/Mg^{2+} sites) are occupied by Mg^{2+} ions that must vacate the sites before Ca^{2+} can bind (Haiech *et al.* 1979; Eberhard & Erne, 1994). Given that $[Mg^{2+}]_{free}$ in the cytosol is around 1 mM, the Ca^{2+}-binding properties of PV are comparable to those of EGTA (Naraghi, 1997; Morris *et al.* 1999; Nagerl *et al.* 2000) (Table 1).

In comparison to PV, few quantitative data are available for CR. Based on observations that CR is sufficiently fast

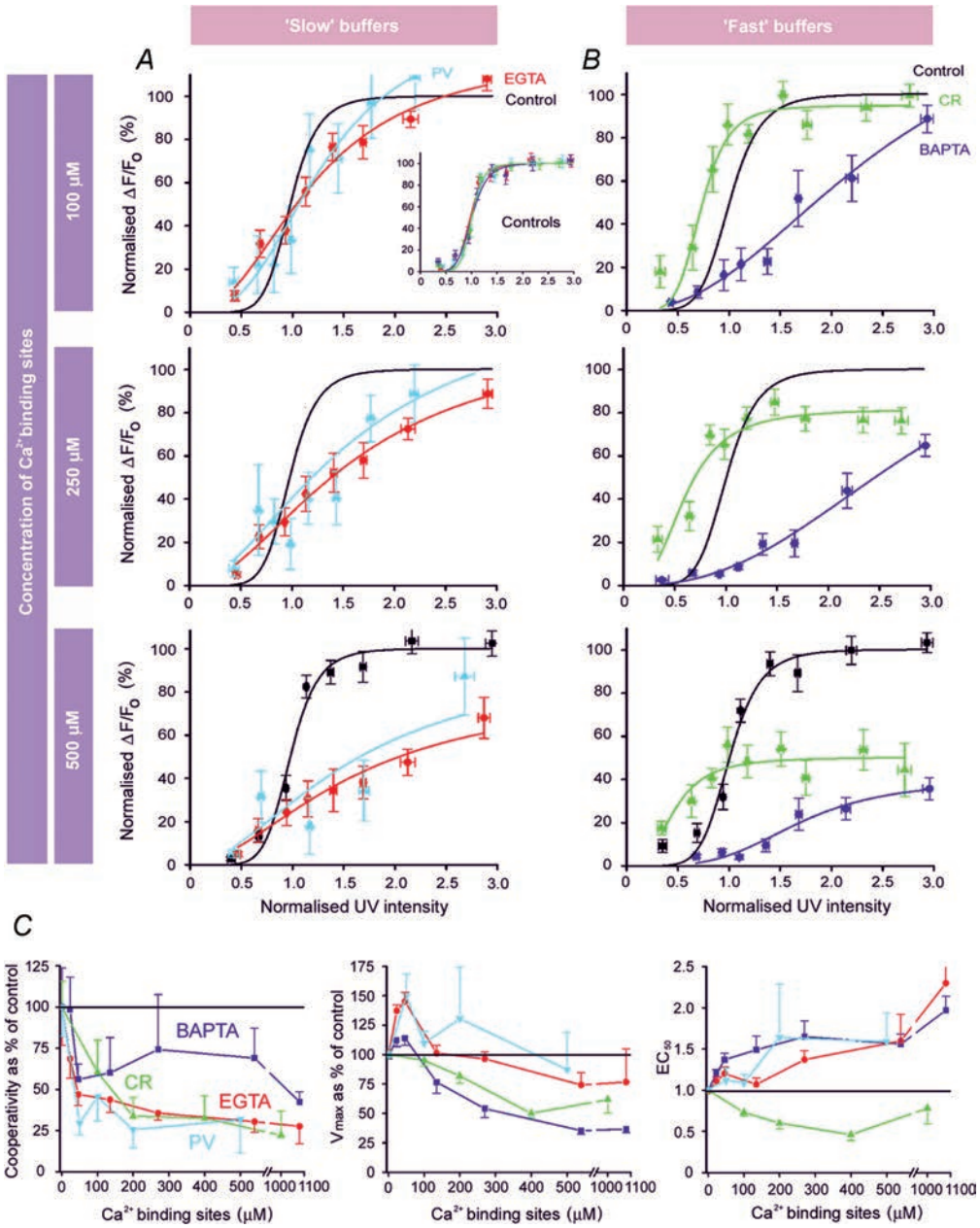

Figure 7. Comparison of actions of synthetic Ca^{2+} buffers and CaBPs on IP_3-evoked Ca^{2+} signals
Graphs summarize data obtained using PV (light blue) and CR (green), together with data taken from Dargan & Parker (2003) obtained previously using EGTA (red) and BAPTA (dark blue). In order to facilitate comparison, buffer concentrations are expressed as the equivalent concentration of Ca^{2+} binding sites (see text for further explanation). Further, all fluorescence data are scaled relative to the maximum of the peak signal obtained at high [IP_3] before loading buffer. Control measurements (before loading buffer) are indicated in black. Different batches of control oocytes were used for each buffer, but the inset plot in *A* shows that normalized control data from these four groups matched closely. For clarity, control data points are shown only in the lower panels of *A* and *B*, and the fitted control Hill curves are replicated in the other panels. *A*, plots show the peak amplitude of Ca^{2+} signals as a function of normalized photolysis flash duration for three different concentrations of slow buffers (EGTA and PV). *B*, corresponding concentration–response relationships for the 'fast' buffers BAPTA and CR. *C*, data derived from the Hill curves in *A* and *B* showing changes in apparent cooperativity of IP_3 action, V_{max} and EC_{50} as a result of increasing concentrations of buffers. Horizontal black lines mark control values in the absence of added buffer. Hill coefficients varied between about 4.5 and 10.5 among the different batches of control oocytes, and the cooperativity is therefore expressed as a percentage of that in each respective control group. Similarly, values of V_{max} are scaled as a percentage of each control group.

to influence presynaptic Ca^{2+} signalling (Edmonds *et al.* 2000) we assumed (Table 1) that its Ca^{2+}-binding kinetics would be comparable to those of BAPTA. However, this is likely to be an oversimplification. In contrast to the single binding site of BAPTA, CR contains five Ca^{2+}-binding sites which – by analogy with a closely related protein calbindin D-28k (Nagerl *et al.* 2000) – are likely to possess different binding properties and may display cooperative rather than independent binding (G. Faas, unpublished observation).

Actions of CaBP and exogenous buffers on IP_3-evoked Ca^{2+} signalling in oocytes

To facilitate comparison between the actions of endogenous CaBP and those of exogenous synthetic Ca^{2+} buffers, we present in Fig. 7 a summary of the present results overlaid with results from Dargan & Parker (2003) obtained using EGTA and BAPTA. Data are grouped comparing slow (EGTA and PV) and fast (BAPTA and CR) buffers. Moreover, concentrations of buffers are normalized by expressing them as the equivalent concentration of functional binding sites. For example, 100 μM EGTA, which has a single binding site, corresponds to 100 μM binding sites; whereas 100 μM CR, with five functional sites (Stevens & Rogers, 1997), is equivalent to 500 μM.

Considering first the slow buffers, PV has actions that are both qualitatively and quantitatively almost identical to EGTA. Both caused IP_3-evoked Ca^{2+} signals to become short-lived, and 'balkanize' Ca^{2+} liberation, such that individual release sites function autonomously to generate discrete puffs. Furthermore, equivalent concentrations of each molecule result in closely similar changes in the concentration–response relationship for IP_3 (Fig. 7*A*), and in parameters derived from Hill fits to these relationships (Fig. 7*C*).

The case with fast buffers is more complex. The effects of CR in some respects resemble those of BAPTA, in that both promote spatially diffuse and slowly decaying Ca^{2+} signals at high $[IP_3]$, reduce the apparent cooperativity for IP_3 action, and diminish the amplitude of responses to maximal $[IP_3]$ (Fig. 7*C*). In other regards, however, CR and BAPTA differ considerably. CR uniquely potentiates responses to low $[IP_3]$, causing a leftward shift in the concentration–response relationship (Fig. 7*B*) and a corresponding decrease in EC_{50} (Fig. 7*C*). Moreover, these responses at low $[IP_3]$ are evident as localized Ca^{2+} puffs, whereas we never observed local signals in the presence of BAPTA (Dargan & Parker, 2003).

Mechanisms of CaBP action on IP_3/Ca^{2+} signalling

Under physiological conditions, PV has an on-rate (k_{on}) comparable to EGTA: thus, a Ca^{2+} ion can diffuse about 1 μm in the presence of 100 μM PV before it is captured (Dargan & Parker, 2003). PV should therefore be capable of disrupting Ca^{2+} communication whilst sparing short-range *intra*cluster Ca^{2+} feedback (Roberts, 1994; Horne & Meyer, 1997; Song *et al.* 1998; Callamaras *et al.* 1998*a*,*b*; Kidd *et al.* 1999). By virtue of its slow binding kinetics, PV is expected to render captured Ca^{2+} ions unavailable for CICR for prolonged periods (Falcke, 2003) (t_{dwell} ~1 s), during which time it can shuttle them long distances ($d_{shuttle}$ = 16 μm) before 'dumping' them deep in the interior of the oocyte where release sites are absent (Callamaras & Parker, 1999). The overall effect of PV would therefore be to functionally uncouple neighbouring clusters by reducing free $[Ca^{2+}]$ between them, thus sharply restricting Ca^{2+} signals around individual release sites. In agreement, PV strongly inhibited Ca^{2+} waves, dissociating global IP_3-evoked Ca^{2+} signals into discrete, localized Ca^{2+} release events (John *et al.* 2001; Figs 5 and 6). Associated with this, the apparent cooperativity for IP_3-evoked Ca^{2+} liberation decreased markedly – with a Hill coefficient reducing from ~7 to ~2 at high [PV] – suggesting that CICR between clusters contributes markedly to the cooperativity under normal conditions, and that the binding of two (or possibly one) molecule of IP_3 to the tetrameric IP_3R is sufficient for channel opening (Dargan & Parker, 2003).

As with EGTA, PV caused a marked acceleration in decay of global Ca^{2+} signals – an effect that appears to arise because both of these slow buffers inhibit a slow tail of Ca^{2+} liberation that lingers during the falling phase of a wave. We had previously proposed that this slow tail component of Ca^{2+} liberation is maintained by cluster–cluster interactions, precisely because it was inhibited by a slow buffer that was expected to disrupt such interactions. However, the present finding (Fig. 6) that puffs normally show a biphasic decay in the absence of added buffer, and that the slow tail component is abolished by PV (but not CR), suggest that the prolonged phase of Ca^{2+} liberation may also involve the properties of the IP_3 receptors themselves, or their interactions within a cluster.

Interpretation of the actions of CR is more difficult, both because this 'fast' CaBP did not simply mimic the actions of the stereotypical fast buffer BAPTA (Dargan & Parker, 2003), and because of the complex and poorly characterized Ca^{2+}-binding kinetics and other properties of CR. In the case of BAPTA we had proposed that it binds Ca^{2+} ions diffusing over nanometer distances within an

IP_3R cluster, thereby disrupting CICR between individual IP_3Rs, and subsequently facilitates Ca^{2+} communication between clusters by rapidly shuttling Ca^{2+} ions over distances of a few micrometres (Dargan & Parker, 2003). However, this scheme would not account for the specific abilities of CR to balkanize Ca^{2+} signals as individual puffs at low $[IP_3]$ as discussed above, nor to sensitize responses to low $[IP_3]$. Even though the fast site(s) of CR are believed to have roughly comparable on-rate(s) (k_{on}) for Ca^{2+} binding to BAPTA (Edmonds *et al.* 2000; Table 1), other sites are probably much slower and may at least partly account for these differences. Moreover, the actions of CR may be further complicated if a fraction of this CaBP is immobilized (Winsky & Kuznicki, 1995; Hubbard & McHugh, 1995) and if CR shows cooperative Ca^{2+} binding. Finally, we cannot exclude the possibility that CR may interact directly with IP_3Rs to modulate their functioning, as described for calmodulin-like neuronal Ca^{2+}-binding proteins (Yang *et al.* 2002; Kasri *et al.* 2003). Clearly, a detailed kinetic characterization of CR and other complex CaBPs will be needed before we can hope to elucidate the mechanistic basis of their varying actions on IP_3-evoked Ca^{2+} signals.

Physiological implications

Our findings highlight the importance of CaBPs in shaping the spatiotemporal properties of IP_3-evoked Ca^{2+} signals – effects that are more complex than for signals arising from a fixed 'pulse' of Ca^{2+} as with Ca^{2+} entry through voltage-gated channels (e.g. Lee *et al.* 2000*a*). CaBPs (such as PV and CR) are found in mammalian cells at concentrations ranging from 50 μM to 2 mM (Plogmann & Celio, 1993; Schwaller *et al.* 2002). We show that PV and CR, even at concentrations (25–250 μM) at the lower end of this range, strongly influence IP_3-mediated Ca^{2+} signalling in the *Xenopus* oocyte model cell system. Most importantly, PV and CR produce specific and strikingly different effects that may arise largely because differences in their binding kinetics confer differential actions on CICR within and between clusters of IP_3Rs. Our results suggest that the concentration and buffering kinetics of CaBPs expressed by a cell are important for tuning the spatiotemporal properties of both local and global IP_3-evoked Ca^{2+} signals, as well as determining the sensitivity and cooperativity of IP_3 action and for conferring a threshold for the ability of the cell to transition from a local to a global mode of Ca^{2+} signalling. It is therefore highly likely that cell-specific expression of CaBPs may serve to shape intracellular Ca^{2+} signals for specific physiological roles. Moreover, although our results concern only IP_3-evoked signals, it should be noted that ryanodine receptors (RyRs), the other major type of intracellular Ca^{2+} release channel, also communicate via CICR (Berridge, 1997), and may therefore be susceptible to similar 'shaping' by CaBPs.

References

Allbritton NL, Meyer T & Stryer L (1992). Range of messenger action of calcium ion and inositol 1,4,5-trisphosphate. *Science* **258**, 1812–1815.

Andressen C, Blumcke I & Celio MR (1993). Calcium-binding proteins: selective markers of nerve cells. *Cell Tissue Res* **271**, 181–208.

Baimbridge KG, Celio MR & Rogers JH (1992). Calcium binding proteins in the nervous system. *Trends Neurosci* **15**, 303–308.

Berridge MJ (1997). Elementary and global aspects of calcium signalling. *J Physiol* **499**, 291–306.

Berridge MJ, Lipp P & Bootman MD (2000). The versatility and universality of calcium signalling. *Nat Rev Mol Cell Biol* **1**, 11–21.

Bezprozvanny I, Watras J & Ehrlich BE (1991). Bell-shaped calcium-response curves of $Ins(1,4,5)P_3$- and calcium-gated channels from endoplasmic reticulum of cerebellum. *Nature* **351**, 751–754.

Bootman M, Niggli E, Berridge M & Lipp P (1997). Imaging the hierarchical Ca^{2+} signalling system in HeLa cells. *J Physiol* **499**, 307–314.

Callamaras N, Marchant JS, Sun XP & Parker I (1998*a*). Activation and co-ordination of $InsP_3$-mediated elementary Ca^{2+} events during global Ca^{2+} signals in *Xenopus* oocytes. *J Physiol* **509**, 81–91.

Callamaras N & Parker I (1998). Caged inositol 1,4,5-trisphosphate for studying release of Ca^{2+} from intracellular stores. *Meth Enzymol* **291**, 380–403.

Callamaras N & Parker I (1999). Radial localization of inositol 1,4,5-trisphosphate-sensitive Ca^{2+} release sites in *Xenopus* oocytes resolved by axial confocal linescan imaging. *J General Physiol* **113**, 199–213.

Callamaras N, Sun XP, Ivorra I & Parker I (1998*b*). Hemispheric asymmetry of macroscopic and elementary calcium signals mediated by $InsP_3$ in *Xenopus* oocytes. *J Physiol* **511**, 395–405.

Cheung WY (1980). Calmodulin plays a pivotal role in cellular regulation. *Science* **207**, 19–27.

Dargan SL & Parker I (2003). Buffer kinetics shape the spatiotemporal patterns of IP_3-evoked Ca^{2+} signals. *J Physiol*; DOI: 10.1113/jphysiol.2003.054247.

Dawson SP, Keizer J & Pearson JE (1999). Fire-diffuse-fire model of dynamics of intracellular calcium waves. *Proc Natl Acad Sci U S A* **96**, 6060–6063.

Eberhard M & Erne P (1994). Calcium and magnesium binding to rat parvalbumin. *Eur J Biochem* **222**, 21–26.

Edmonds B, Reyes R, Schwaller B & Roberts WM (2000). Calretinin modifies presynaptic calcium signalling in frog saccular hair cells. *Nat Neurosci* **3**, 786–790.

Falcke M (2003). Buffers and oscillations in intracellular Ca^{2+} dynamics. *Biophys J* **84**, 28–41.

Fill M & Copello JA (2002). Ryanodine receptor calcium release channels. *Physiol Rev* **82**, 893–922.

Finch EA, Turner TJ & Goldin SM (1991). Calcium as a coagonist of inositol 1,4,5-trisphosphate-induced calcium release. *Science* **252**, 443–446.

Haiech J, Derancourt J, Pechere JF & Demaille JG (1979). Magnesium and calcium binding to parvalbumins: evidence for differences between parvalbumins and an explanation of their relaxing function. *Biochemistry* **18**, 2752–2758.

Hirota J, Michikawa T, Miyawaki A, Furuichi T, Okura I & Mikoshiba K (1995). Kinetics of calcium release by immunoaffinity-purified inositol 1,4,5-trisphosphate receptor in reconstituted lipid vesicles. *J Biol Chem* **270**, 19046–19051.

Horne JH & Meyer T (1997). Elementary calcium-release units induced by inositol trisphosphate. *Science* **276**, 1690–1693.

Hubbard MJ & McHugh NJ (1995). Calbindin 28kDa and calbindin 30kDa (calretinin) are substantially localised in the particulate fraction of rat brain. *FEBS Lett* **374**, 333–337.

Iino M (1990). Biphasic Ca^{2+} dependence of inositol 1,4,5-trisphosphate-induced Ca^{2+} release in smooth muscle cells of the guinea pig *taenia caeci*. *J General Physiol* **95**, 1103–1122.

John LM, Mosquera-Caro M, Camacho P & Lechleiter JD (2001). Control of IP_3-mediated Ca^{2+} puffs in *Xenopus laevis* oocytes by the Ca^{2+}-binding protein parvalbumin. *J Physiol* **535**, 3–16.

Kasri NN, Holmes AM, Bultynck G, Parys JB, Bootman MD, Rietdorf K, Missiaen L, *et al.* (2003). Regulation of $InsP_3$ receptor activity by neuronal Ca^{2+}-binding proteins. *EMBO J*; PMID: 14685260.

Kidd JF, Fogarty KE, Tuft RA & Thorn P (1999). The role of Ca^{2+} feedback in shaping $InsP_3$-evoked Ca^{2+} signals in mouse pancreatic acinar cells. *J Physiol* **520**, 187–201.

Lechleiter JD & Clapham DE (1992). Molecular mechanisms of intracellular calcium excitability in *X. laevis* oocytes. *Cell* **69**, 283–294.

Lee SH, Rosenmund C, Schwaller B & Neher E (2000*a*). Differences in Ca^{2+} buffering properties between excitatory and inhibitory hippocampal neurons from the rat. *J Physiol* **525**, 405–418.

Lee SH, Schwaller B & Neher E (2000*b*). Kinetics of Ca^{2+} binding to parvalbumin in bovine chromaffin cells: implications for $[Ca^{2+}]$ transients of neuronal dendrites. *J Physiol* **525**, 419–432.

Mak DO, McBride S & Foskett JK (1998). Inositol 1,4,5-trisphosphate activation of inositol trisphosphate receptor Ca^{2+} channel by ligand tuning of Ca^{2+} inhibition. *Proc Natl Acad Sci U S A* **95**, 15821–15825.

Marchant JS & Parker I (2000). Functional interactions in Ca^{2+} signalling over different time and distance scales. *J General Physiol* **116**, 691–696.

Marchant JS & Taylor CW (1997). Cooperative activation of IP_3 receptors by sequential binding of IP_3 and Ca^{2+} safeguards against spontaneous activity. *Curr Biol* **7**, 510–518.

Meinrenken CJ, Borst GG & Sakmann B (2003). Local routes revisited: the space and time dependence of the Ca^{2+} signal for phasic transmitter release at the rat calyx of Held. *J Physiol* **547**, 665–689.

Meyer T, Wensel T & Stryer L (1990). Kinetics of calcium channel opening by inositol 1,4,5-trisphosphate. *Biochemistry* **29**, 32–37.

Morris SA, Correa V, Cardy TJ, O'Beirne G & Taylor CW (1999). Interactions between inositol trisphosphate receptors and fluorescent Ca^{2+} indicators. *Cell Calcium* **25**, 137–142.

Nagerl UV, Novo D, Mody I & Vergara JL (2000). Binding kinetics of calbindin-D(28k) determined by flash photolysis of caged Ca^{2+}. *Biophys J* **79**, 3009–3018.

Naraghi M (1997). T-jump study of calcium binding kinetics of calcium chelators. *Cell Calcium* **22**, 255–268.

Neher E (2000). Calcium buffers in flash-light. *Biophys J* **79**, 2783–2784.

Parker I, Callamaras N & Wier WG (1997). A high-resolution, confocal laser-scanning microscope and flash photolysis system for physiological studies. *Cell Calcium* **21**, 441–452.

Parker I, Yao Y & Ilyin V (1996). Fast kinetics of calcium liberation induced in Xenopus oocytes by photoreleased inositol trisphosphate. *Biophys J* **70**, 222–237.

Parys JB, Sernett SW, DeLisle S, Snyder PM, Welsh MJ & Campbell KP (1992). Isolation, characterization, and localization of the inositol 1,4,5-trisphosphate receptor protein in *Xenopus laevis* oocytes. *J Biol Chem* **267**, 18776–18782.

Pauls T, Drussel J, Cox JA, Clark ID, Szabo AG, Gange SM, Sykes BD & Berchtold MW (1993). Metal binding properties of recombinant rat parvalbumin wild-type and F102W mutant. *J Biol Chem* **268**, 20897–20903.

Plogmann D & Celio MR (1993). Intracellular concentration of parvalbumin in nerve cells. *Brain Res* **600**, 273–279.

Roberts WM (1994). Localization of calcium signals by a mobile calcium buffer in frog saccular hair cells. *J Neurosci* **14**, 3246–3262.

Schmidt H, Brown EB, Schwaller B & Eilers J (2003*a*). Diffusional mobility of parvalbumin in spiny dendrites of cerebellar Purkinje neurons quantified by fluorescence recovery after photobleaching. *Biophys J* **84**, 2599–2608.

Schmidt H, Stiefel KM, Racay P, Schwaller B & Eilers J (2003*b*). Mutational analysis of dendritic Ca^{2+} kinetics in cerebellar Purkinje cells: role of parvalbumin and calbindin D28k. *J Physiol* **551**, 13–32.

Schwaller B, Durussel I, Jermann D, Herrmann B & Cox JA (1997). Comparison of the Ca^{2+} binding properties of human recombinant calretinin-22k and calretinin. *J Biol Chem* **272**, 29663–29671.

Schwaller B, Meyer M & Schiffmann S (2002). 'New' functions for 'old' proteins: The role of the calcium binding proteins calbindin D-28k, calretinin and parvalbumin, in cerebellar physiology. Studies with knockout mice. *Cerebellum* **1**, 241–258.

Shuai JW & Jung P (2002). Stochastic properties of Ca^{2+} release of inositol 1,4,5-trisphosphate receptor clusters. *Biophys J* **83**, 87–97.

Shuai JW & Jung P (2003). Optimal ion channel clustering for intracellular calcium signalling. *Proc Natl Acad Sci U S A* **100**, 506–510.

Simpson PB, Mehotra S, Lange GD & Russell JT (1997). High density distribution of endoplasmic reticulum proteins and mitochondria at specialized Ca^{2+} release sites in oligodendrocyte processes. *J Biol Chem* **272**, 22654–22661.

Song LS, Sham JS, Stern MD, Lakatta EG & Cheng H (1998). Direct measurement of SR release flux by tracking 'Ca^{2+} spikes' in rat cardiac myocytes. *J Physiol* **512**, 677–691.

Stern MD (1992). Buffering of calcium in the vicinity of a channel pore. *Cell Calcium* **13**, 183–192.

Stevens J & Rogers JH (1997). Chick calretinin: purification, composition, and metal binding activity of native and recombinant forms. *Protein Expr Purif* **9**, 171–181.

Sun XP, Callamaras N, Marchant JS & Parker I (1998). A continuum of InsP_3-mediated elementary Ca^{2+} signalling events in *Xenopus* oocytes. *J Physiol* **509**, 67–80.

Swillens S, Dupont G, Combettes L & Champeil P (1999). From calcium blips to calcium puffs: theoretical analysis of the requirements for interchannel communication. *Proc Natl Acad Sci U S A* **96**, 13750–13755.

Vetter SW & Leclerc E (2003). Novel aspects of calmodulin target recognition and activation. *Eur J Biochem* **270**, 404–414.

Winsky L & Kuznicki J (1995). Distribution of calretinin, calbindin D28k and parvalbumin in subcellular fractions of rat cerebellum: effects of calcium. *J Neurochem* **65**, 381–388.

Yang J, McBride S, Mak DO, Vardi N, Palczewski K, Haeseleer F & Foskett JK (2002). Identification of a family of calcium sensors as protein ligands of inositol trisphosphate receptor Ca^{2+} release channels. *Proc Natl Acad Sci U S A* **99**, 7711–7716.

Yao Y, Choi J & Parker I (1995). Quantal puffs of intracellular Ca^{2+} evoked by inositol trisphosphate in *Xenopus* oocytes. *J Physiol* **482**, 533–553.

Acknowledgements

We thank Brian Edmonds, Silvina Ponce-Dawson and John Pearson for helpful discussions, and Elaine Fisher for writing custom image acquisition software. This research was funded by NIH grants GM48071 and GM58329 (to I.P.) and by Swiss National Science Foundation grants 3100-063448.00/1 and 3100A0-100400/1 (to B.S.).